# Lattice effects and magnetic structure in the layered colossal magnetoresistance manganite $La_{2-2x}Sr_{1+2x}Mn_2O_7$, $x=0.3$

D. N. Argyriou
*Los Alamos Neutron Science Center, Los Alamos National Laboratory, Los Alamos, New Mexico 87545*

J. F. Mitchell
*Materials Science Division, Argonne National Laboratory, Argonne, Illinois 60439*

P. G. Radaelli
*ISIS Facility, Rutherford Appleton Laboratory, Chilton 0X11 0QX, United Kingdom*

H. N. Bordallo
*Los Alamos Neutron Science Center, Los Alamos National Laboratory, Los Alamos, New Mexico 87545*

D. E. Cox
*Brookhaven National Laboratory, Upton, New York 11973*

M. Medarde and J. D. Jorgensen
*Materials Science Division, Argonne National Laboratory, Argonne, Illinois 60439*

(Received 18 September 1998)

We report on the temperature dependence of the crystal and magnetic structure of the layered colossal magnetoresistive manganite, $La_{2-2x}Sr_{1+2x}Mn_2O_7$, $x=0.3$. Neutron-diffraction measurements show that the insulator-metal (IM) transition ($T_{IM}$) at ~100 K is accompanied by a ferromagnetic (FM) ordering of spins within $MnO_6$ bilayers (*intrabilayer* coupling), but with an antiferromagnetic coupling between neighboring bilayers (*interbilayer* coupling). Below $T_{IM}$, the Mn spins rotate from ~45° inclination to the *c* axis until they are almost parallel to the *c* axis at 5 K. Coincident with this spin reorientation, a FM *c* axis component develops below 75 K. Evidence from both neutron and synchrotron x-ray-diffraction experiments suggest that the FM *c*-axis magnetic moment results from a second layered manganite phase with composition $0.3 \lesssim x \lesssim 0.32$. This observation emphasizes the need for thorough examination of the homogeneity when measuring bulk properties (e.g., magnetization, transport) of nominally $x=0.3$ samples. Associated with the electronic and magnetic transitions, a pronounced lattice response along the *c* axis (observed in both phases) signals a transfer of charge into $d_{x^2-y^2}$ orbitals in the low-temperature phase. That the lattice effects here are opposite in sign to those observed in the $x=0.4$ layered manganite points to the sensitivity of the spin-lattice-charge coupling to dopant concentration in these reduced-dimensionality manganites. [S0163-1829(99)00513-5]

## I. INTRODUCTION

Naturally layered manganite perovskites that exhibit colossal magnetoresistance[1–3] (CMR) have provided the opportunity not only to study the strong interplay among charge, spin, and lattice in reduced dimensions, but also to explore phenomena that are not found in the three-dimensional (3D) perovskite manganites. For example, the natural stacking of $(Ln,Sr)MnO_3$ perovskite layers, separated by (La,Sr)O blocking layers, forms the framework of tunneling structures and spin valves in a single chemical phase, as opposed to the larger scale structures obtained by thin-film deposition. Exploring these opportunities, Kimura *et al.*[1,2] have recently reported the observation of spin-polarized interlayer conductivity and high CMR in the naturally layered materials $La_{2-2x}Sr_{1-2x}Mn_2O_7$, $x=0.3$ ($10^4$% at 50 kOe and at 90 K). From magnetization measurements they suggest that this layered manganite orders ferromagnetically (FM) along the *c* axis at 90 K, but below 60 K an anomaly in the magnetization suggests the development of canted interlayer antiferromagnetism (AF). This is in contrast to the ferromagnetic coupling observed in the previously studied $x=0.4$ compound.[4] This AF coupling is believed to be responsible for the large tunneling magnetoresistance (TMR) observed in the *c*-axis transport at low temperatures.[1–3] Furthermore, Kimura *et al.*[1,2] demonstrated that the magnetic coupling between perovskite layers may be manipulated with magnetic field or pressure; application of a magnetic field produces an increased interlayer conductivity while hydrostatic pressure decreases the conductivity along the *c* axis and within the *ab* plane.[2] This behavior has likewise been linked to a proposed AF structure.

Such a combination of FM planes with AF coupling is observed in the canonical A-type antiferromagnet, $LaMnO_3$, which is an insulator. However, Akimoto *et al.*[5] have reported that $La_{0.46}Sr_{0.54}MnO_3$ exhibits a metallic state and type-A antiferromagnetism. In addition, they have suggested that quasi-2D metallic conductivity in $La_{0.46}Sr_{0.54}MnO_3$ oc-

 

curs in the planes via double exchange in $d_{x^2-y^2}$ bands, while super exchange dominates along the *z* axis. This may be possible due to a high anisotropy between $d_{x^2-y^2}$ and $d_{3z^2-r^2}$ orbitals found in this perovskite manganite.[5] Thus, the present bilayer compound can be regarded as an extension of this perovskite into reduced dimensions.

In this paper we report on the lattice effects and accompanying magnetic ordering in $La_{2-2x}Sr_{1-2x}Mn_2O_7$, with a nominal dopant concentration of $x=0.3$. We find that associated with a sharp drop in resistivity both within the *ab* plane and along the *c* axis, Mn moments order to form ferromagnetic perovskite bilayers that are antiferromagnetically coupling along the *c* axis; at low temperatures we find a magnetic structure similar to that suggested by Kimura *et al.*[2] However, in addition to this AF interlayer coupling, we find a rich magnetic behavior characterized by rotating Mn moments and coexisting AF and FM interbilayer coupling. Both crystal structure data from high-resolution synchrotron x-ray diffraction and magnetic structure data from neutron diffraction indicate that the latter effect is attributable to the coexistance of two $n=2$ layered phases in the sample whose dopant concentrations are extremely close ($0.3 \lesssim x \lesssim 0.32$). The temperature dependence of the lattice parameters for both phases is qualitatively the same, indicating that the charge-spin-lattice interactions are similar in both phases. Despite the small difference in dopant concentration, there is a dramatic difference in magnetic structure: the hole-poor phase exhibits AF interbilayer coupling and the hole-rich phase FM interbilayer coupling. As found in other manganites, lattice effects accompany the magnetic/electronic transition. In the $x=0.3$ sample a strong *c*-axis contraction observed on cooling through $T_N$ tracks the change in the apical Mn-O bonds. This behavior is consistent with a charge transfer into $d_{x^2-y^2}$ orbitals. In contrast, the *a* axis is very weakly temperature dependent, and the anomaly at 80 K is presumably attributable solely to magnetostrictive effects, as it is quite small ($\Delta a/a \sim 0.03\%$), and it tracks the projection of the ordered moment on to the *ab* plane. These lattice effects are opposite to those found in the previously studied $x=0.4$ material,[4] suggesting that charge-lattice coupling at the magnetic transition is different at these two dopant levels.

## II. EXPERIMENTAL DETAILS AND SAMPLE CHARACTERIZATION

Single crystals of $La_{2-2x}Sr_{1+2x}Mn_2O_7$ were melt grown on flowing 100% $O_2$ in a floating zone optical image furnace (NEC SC-M15HD). Crystals were characterized using inductively coupled plasma (ICP) analysis, yielding an *average* composition of $x=0.30(1)$. Transport measurements on a small specimen from this crystal boule show a peak in both $\rho_{ab}$ and $\rho_c$ at $T_{IM} \sim 100$ K. Details of these transport measurements are reported elsewhere.[6] This transport behavior is qualitatively similar to that observed by Kimura *et al.* on a $x=0.3$ specimen below 100 K.[1,2] Sections from various locations of the as-grown boule (but not from the ends) were pulverized and used in powder-diffraction studies. The same pulverized crystalline samples (~3 g) was used in all x-ray and neutron powder-diffraction measurements. The quality (chemical phase homogeneity) of the powdered crystalline samples was investigated as a function of temperature (20–300 K) using high-resolution x-ray diffraction, performed at beam line X7A at the National Synchrotron Light Source (NSLS) at the Brookhaven National Laboratory, using a wavelength of 0.8 Å and a Ge(111)/Ge(220) monochromator/analyzer combination. The temperature dependence of the crystal structure was also studied between 20 and 300 K using the Special Environment Powder Diffractometer (SEPD) at Argonne's Intense Pulsed Neutron Source. The magnetic structure was determined using the high-flux diffractometer D20 operated at the Institute Laue-Langevin ($\lambda=2.41$ Å, $2\theta=0$–$160°$) between 5–150 K.

TABLE I. Results of Rietveld refinement for $La_{2-2x}Sr_{1+2x}Mn_2O_7$, $x=0.3$ from neutron powder-diffraction data collected on SEPD at 300 K. The space group used in the refinement was *I4/mmm*, $a=3.861\,82(3)$ Å and $c=20.3544(3)$ Å. Site occupancies are given as a fractional occupancy where a value of 1 indicates full occupation. For the Mn site the occupancy was fixed to 1. $wRp=6.15\%$, goodness of fit=1.8, $R(F^2)=3.5\%$, $U[\mathrm{La,Sr(1)}]=U[\mathrm{La,Sr(2)}]$.

| Atom | *x* | *y* | *z* | Occupancy | *U* (Å$^2$) |
|---|---|---|---|---|---|
| La,Sr(1) | 0 | 0 | 1/2 | 1.01(1) | 0.0078(2) |
| La,Sr(2) | 0 | 0 | 0.3169(1) | 0.97(1) | 0.0078(2) |
| Mn | 0 | 0 | 0.0969(2) | 1 (fixed) | 0.0041(4) |
| O(1) | 0 | 0 | 0 | 1.00(2) | $U_{11}=0.013(1)$ |
| | | | | | $U_{33}=0.014(2)$ |
| O(2) | 0 | 0 | 0.1973(1) | 1.01(1) | $U_{11}=0.014(1)$ |
| | | | | | $U_{33}=0.021(1)$ |
| O(3) | 0 | 1/2 | 0.0955(8) | 1.01(2) | $U_{11}=0.007(1)$ |
| | | | | | $U_{22}=0.006(1)$ |
| | | | | | $U_{33}=0.019(10)$ |

Neutron-diffraction data were consistent with a tetragonal cell, space group *I4/mmm*, as we have reported earlier for the $x=0.4$ composition;[4] however, two additional phases were observed in small amounts: perovskite (3 wt %) and single layer $(La,Sr)_2MnO_4$ (4 wt %). These second phases are typically found in an annulus at the outer regions of the boule. Results of structural analysis using the Rietveld method at room temperature are given in Table I. These refinements indicate that the occupancy of the oxygen sublattice is fully stoichiometric, as is the 12-coordinate La,Sr(1) site within the perovskite bilayer. However, the fractional occupancy of the 9-coordinate La,Sr(2) site in the rocksalt layer is less than unity, suggesting the presence of either cation vacancies for this specific site [3(1)%], or a deviation from the nominal La/Sr ratio. A 3% vacancy concentration on the La,Sr(2) site would give the same effect as a 30(10)% excess of Sr in the rocksalt layers.

Battle *et al.*[7] have pointed out that ceramic samples of the $LaSr_2Mn_2O_7$ ($x=0.5$) phase separate into two chemically distinct Ruddlesden-Popper (RP) phases. To investigate this possibility in our sample, we have further characterized it using high-resolution synchrotron x-ray diffraction at the X7A diffractometer at the NSLS ($\Delta d/d \sim 0.005$). The results of this measurement indicate that there are indeed two chemically distinct $n=2$ RP phases in this sample. Considering the $(0,0,l)$ reflections, and the (0,0,10) in particular (Fig. 1), a small asymmetry at *higher* angles is observed that was not resolved in the neutron experiment. This asymmetry is

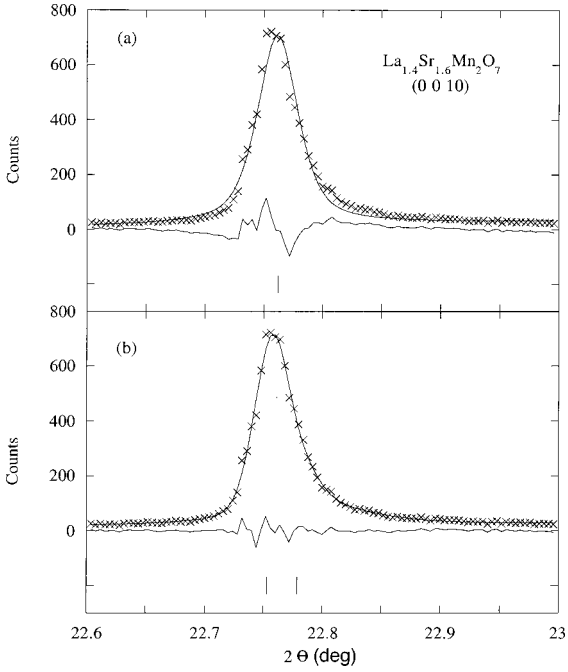


FIG. 1. The (0 0 10) reflection of $La_{2-2x}Sr_{1+2x}Mn_2O_7$ at 20 K (crosses) measured using high-resolution x-ray diffraction on the X7A beam line at the NSLS. The profile is clearly asymmetric with an asymmetric tail at higher angles. The upper panel shows the fit to the data assuming one peak profile ($\chi^2=12$) while the lower panel shows the fit to two peak profiles ($\chi^2=2.2$). The positions of the calculated peaks and the difference between observed and calculated values are shown on the bottom of each panel.

visible at 20 K in several reflections: for example, (0,0,10), (2,0,0), (1,1,10), (2,2,0), and (1,0,17). The observed asymmetry may represent a distribution of $c$ axes that may be modeled in simple terms as multiple $n=2$ RP phases. Indeed, using a series of 16 reflections measured at 20 K we find that the data are well modeled using two $n=2$ RP phases. From this refinement we find a major phase with lattice constants of $a=3.860\,38(6)$ Å and $c=20.2784(3)$, and a minor phase with $a=3.8624(2)$ Å and $c=20.2551(20)$ Å. The proportion of the minor phase is estimated at ~25%. Unfortunately, a more accurate measurement is prevented by the high degree of correlation between the peak shape parameters for the two reflections. The domain size of both phases is macroscopic (>1000 Å), as indicated by the full width at half maximums (FWHM's) of the x-ray reflections: for the (2,0,0) reflection a ~0.02° and ~0.03° FWHM for major and minor phases, respectively; for the (0,0,10) reflection a 0.04° and 0.06° FWHM, again for major and minor phases, respectively.

The temperature dependence of that lattice parameters of the majority and minority phases was determined by analyzing the (2,0,0) and (0,0,10) reflections as a function of temperature. The data in Fig. 2(a) show that both phases have qualitatively the same temperature dependence and that they parallel the temperature dependence obtained from the neutron data [Fig. 2(b)]. At 20 K, the difference in lattice parameters (minor–major) is $\Delta a=0.002$ Å and $\Delta c=-0.026$ Å, much smaller than that reported by Battle *et al.*[7] (e.g., $\Delta a=-0.008$ Å, $\Delta c=0.132$ Å for $LaSr_2Mn_2O_7$). Such small differences are below the resolution of the instruments used in the neutron investigations ($\Delta d/d>0.035$). Because the $c/a$ ratio is expected to decrease with increasing $Mn^{4+}$ concentration (due to the diminishing influence of the Jahn-Teller effect), these differences in lattice parameters for $x=0.3$ are consistent with the majority component having a smaller value of dopant concentration $x$ than the minority component. Lattice parameters for the two distinct chemical phases were refined from the x-ray data up to 300 K, the highest temperature reached. We thus cannot comment on whether the two-phase mixture forms during synthesis or results from a chemical phase separation at some temperature between 300 K and the melting point.

## III. LATTICE EFFECTS AT $T_{IM}$

The parallel variation of the lattice parameters in the majority and minority phases revealed by the x-ray study im-

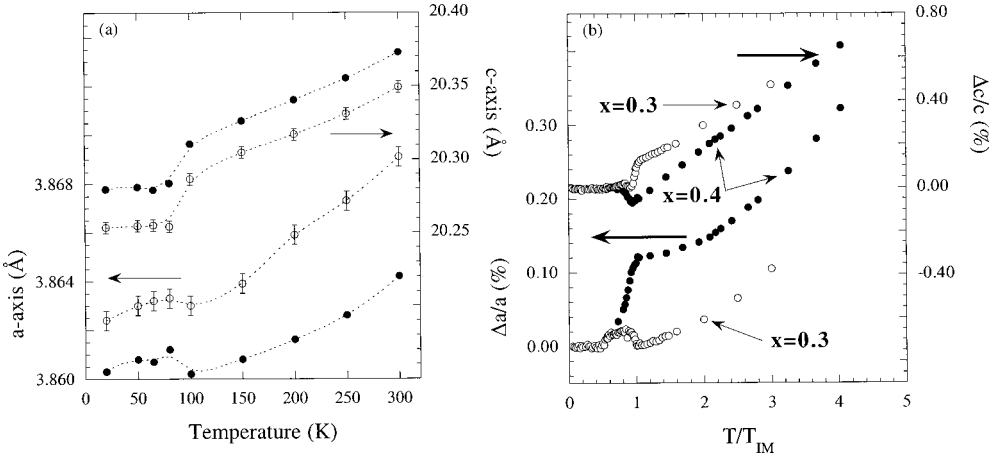


FIG. 2. Lattice parameters as a function of temperature for $La_{2-2x}Sr_{1+2x}Mn_2O_7$, with nominal $x=0.3$. (a) Lattice parameters for the major (open symbols) and minor (filled symbols) phases as a function of temperature as determined from synchrotron x-ray diffraction. (b) Lattice parameters from Rietveld analysis of neutron-diffraction data from $x=0.3$ (open symbols) and $x=0.4$ (filled symbols). For the $x=0.3$ sample lattice parameters were determined from Rietveld analysis of diffraction data from the D20 diffractometer for $T<150$ K and from SEPD between 20–300 K. For $x=0.4$, lattice parameters are taken from Ref. 3. Lattice parameters have been normalized to measurements at 5 K for $x=0.3$ [$a=3.865\,94(11)$ Å, $c=20.299\,69(98)$ Å] and 20 K for $x=0.4$ [$a=3.867\,60(3)$ Å, $c=20.062\,07(27)$ Å)]. Error bars are smaller than the plot symbols. $T_{IM}$ for $x=0.4$ is 125 K.

TABLE II. Mn-O bond lengths at various temperatures.

| Temperature (K) | Mn-O(1) (Å) | Mn-O(2) (Å) | Mn-O(3) (Å) | $\langle$Mn-$O_{apical}\rangle$ (Å) |
|---|---|---|---|---|
| 300 | 1.9716(28) | 2.045(4) | 1.93110(4) | 2.0083(34) |
| 160 | 1.9553(25) | 2.052(4) | 1.92930(6) | 2.0036(33) |
| 100 | 1.9572(29) | 2.043(4) | 1.92901(5) | 2.0001(35) |
| 50 | 1.9568(29) | 2.036(4) | 1.92938(4) | 1.9964(34) |
| 11 | 1.9551(28) | 2.036(4) | 1.92929(5) | 1.9956(34) |

plies that even the ''average'' structure probed by the neutrons qualitatively reflects the behavior of the individual phases. As the neutron data measured on SEPD are more extensive in terms of both Q range and temperatures measured than the x-ray measurements, refinements of these data will be used to discuss the structural evolution with temperature.

Similar to what has been observed in perovskites and in the $x=0.4$ layered material, the $x=0.3$ layered manganite demonstrates pronounced lattice effects (see Fig. 2) at $T_{IM}$. Above $T_{IM}$ both *a* and *c* lattice parameters appear to decrease linearly with decreasing temperature. At $T_{IM}$, the *c* axis contracts by 0.14% while the *a* axis shows a slight expansion ($\sim$0.03%) between 100 and 50 K [see Fig. 2(b)]. The exceedingly small magnitude of the *a*-axis expansion combined with the fact that the *a* axis essentially tracks the development of magnetic order in the *ab* plane (see next section) argues that the origin of this effect is purely magnetostrictive. The changes in lattice parameters at $T_{IM}$ for $x=0.3$ result in an overall volume contraction of $\sim$0.09% (comparable to that of the $x=0.4$ layered manganite and other manganite perovskites[4,8,9]). Interestingly, the *direction* of the lattice effects in this $x=0.3$ is opposite to that of the $x=0.4$ composition.[4,10] In $x=0.4$ materials charge delocalization is accompanied by an abrupt contraction of the *a* axis by 0.16% and an expansion of the *c* axis by $\sim$0.06%.[4,10] The temperature dependence of the $x=0.4$ material is also shown in Fig. 2(b) for comparison. It is not clear why the *a* axis of the $x=0.3$ sample changes by so little compared to $x=0.4$, but the behavior probably reflects a difference in the distribution of charge between these two compositions, which, as we shall discuss below, may result from a difference in their $e_g$ orbital occupations.

The temperature evolution of the three symmetry independent Mn-O bond lengths provides a microscopic view of the lattice response at $T_{IM}$. The largest effects are seen along the *c* direction. Crystallographic parameters computed from Rietveld refinement of neutron powder data for the $x=0.3$ composition at 300 K and several Mn-O bond lengths at various temperatures are given in Table II (the labeling of O atoms used here is shown in Fig. 5(a). Consistent with the temperature dependence of the *a* axis, we find that the Mn-O(3) bond shows a monotonic decrease with temperature from 300 K down to $T_{IM}$. As shown in Fig. 3(a), at $T_{IM}$ Mn-O(3) (and hence the *a* axis) expands slightly; in $x=0.4$ it contracts, and considerably more so than in $x=0.3$. The small anomaly between 100 and 50 K on the *a* axis results from changes in the Mn-O(3) bond length as opposed to the Mn-O(3)-Mn bond angle (as in the $x=0.4$ composition, in

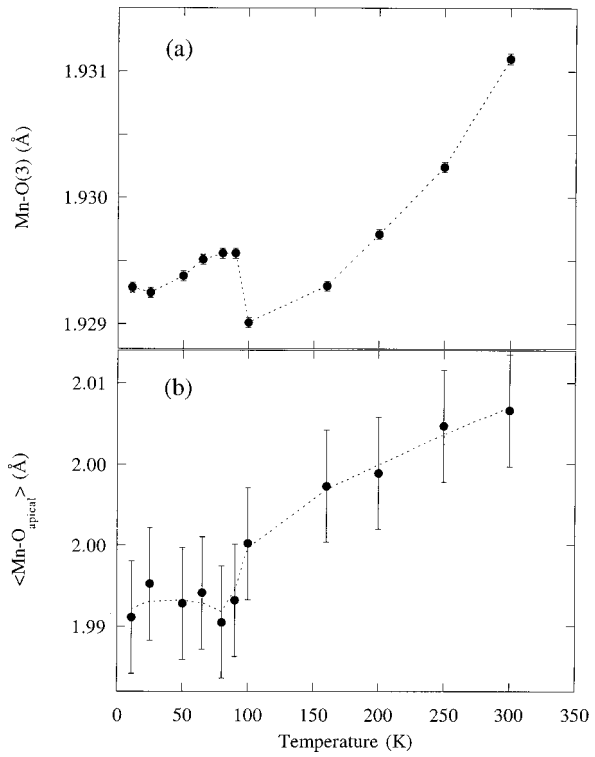


FIG. 3. Temperature dependence of (a) the Mn-O(3) bond lengths and (b) the $\langle$Mn-$O_{apical}\rangle$ bond is given by $\frac{1}{2}$[Mn-O(1)] $+\frac{1}{2}$[Mn-O(2)].

$x=0.3$ the Mn-O(3)-Mn bond angle is $\sim$178.8(5)° and does not vary with temperature, while the Mn-O(1)-Mn bond angle is constrained by symmetry to 180°.[4,10] Although not shown here, the *a* axis varies linearly with the in-plane component of the Mn ordered moment, corroborating the assignment of this lattice parameter variation to magnetostriction.

The more significant changes occur along the *c* axis at $T_{IM}$ and can be understood in terms of the apical Mn-O bonds. Because determining the length of individual apical Mn-O bonds is complicated by the presence of two crystallographic phases in this sample, we look specifically at the average apical Mn-O bond $\langle$Mn-$O_{apical}\rangle$.[11] As shown in Fig. 3(b) the average apical Mn-O bond contracts at $T_{Im}$ by an amount that is approximately the same as the *c* axis contraction. In $x=0.4$, the *c* axis expands at $T_{IM}$ by 0.06%.[4] The opposite behavior of the lattice parameters between the $x=0.3$ and $x=0.4$ compositions also appears in the changes of the Jahn-Teller distortion of the $MnO_6$ octahedra below $T_{IM}$. In the $x=0.4$ composition we reported that the octahedral distortion parameter $D=\langle$Mn-$O_{apical}\rangle$/Mn-$O_{equatorial}$, *increases* by 0.6% at $T_{IM}$ (Fig. 4). However, in this $x=0.3$ material we find that is *decreases* by 0.3% at $T_{IM}$, suggesting that a more highly conductive electronic state is characterized by less distorted $MnO_6$ octahedra at this composition. This finding agrees with the recent pair distribution function analysis of neutron-scattering data from a ceramic $x=0.3$ sample reported by Louca *et al.*[12] The same behavior has also been noted for the manganite perovskites, for it has been widely shown that the octahedral distortion gets smaller—although it remains nonzero—in the metallic regime.[8,9]

The different lattice effects observed in $x=0.4$ and $x=0.3$ cannot be accounted for purely by the change in the mean

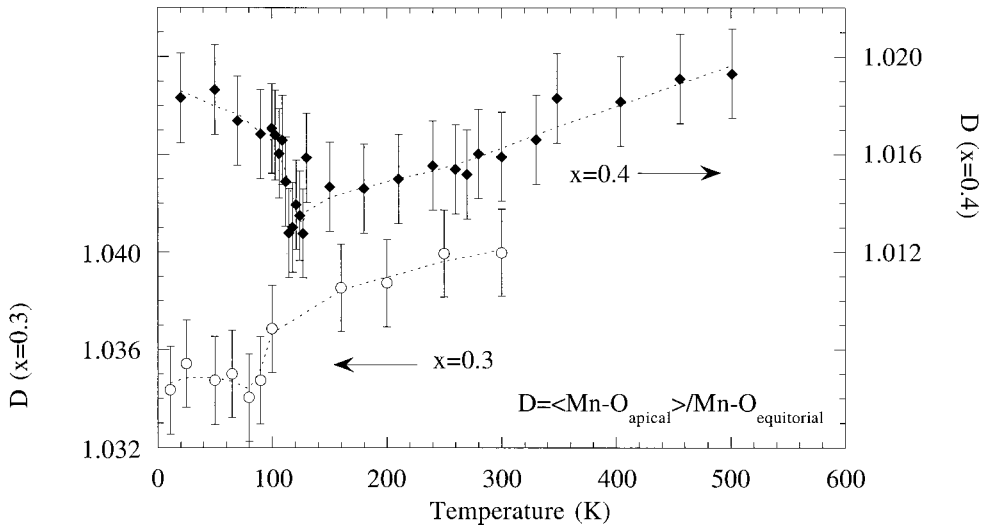


FIG. 4. Variation of the octahedral distortion parameter $D$ as a function of temperature for $x=0.3$ (open circles) and $x=0.4$ (filled circles).

ionic radius of the rare-earth site cation. La and Sr are of similar ionic size so between $x=0.4$ and $x=0.3$ the ionic radius changes by a mere 0.005 Å. This indicates that the direction of the lattice effect at $T_{\mathrm{IM}}$ depends on the electronic doping, which in turn influences the character of the occupied orbitals on the Mn ion. In the $x=0.4$ compound the contraction of the equatorial Mn-O(3) and the expansion of the apical Mn-O(2) bond at $T_{\mathrm{IM}}$ is consistent with a charge transfer from in-plane $d_{x^2-y^2}$ orbitals above $T_C$ to axially directed $d_{3z^2-r^2}$ orbitals below $T_{\mathrm{IM}}$. Recent band structure calculations and ARPES measurements reported by Dessau *et al.*[13] in single crystals of $x=0.4$ material indicate that the $d_{x^2-y^2}$ orbital is slightly lower in energy than $d_{3z^2-r^2}$, but that these bands overlap substantially throughout the Brillouin zone. This near degeneracy of the orbitals indicates that charge transfer between the two orbital manifolds could be a reasonable response of the system to the coupled magnetic-electronic transition. In addition, Zhou *et al.*[14] have suggested that in the $x=0.4$ compound the application of pressure may result in a charge transfer from $d_{x^2-y^2}$ to $d_{3z^2-r^2}$ orbitals in the metallic state, perhaps resulting from this large overlap between $e_g$ electronic states. In contrast, for the $x=0.3$ sample the marked contraction of the $c$ axis on cooling through $T_{\mathrm{IM}}$ results directly from the contraction of the apical Mn-O bonds. This is consistent with a charge transfer from $d_{3z^2-r^2}$ orbitals to the planar $d_{x^2-y^2}$ orbital at $T_{IM}$, just the opposite of what is found in the $x=0.4$ material. In this interpretation the analogy to Akimoto's A-type

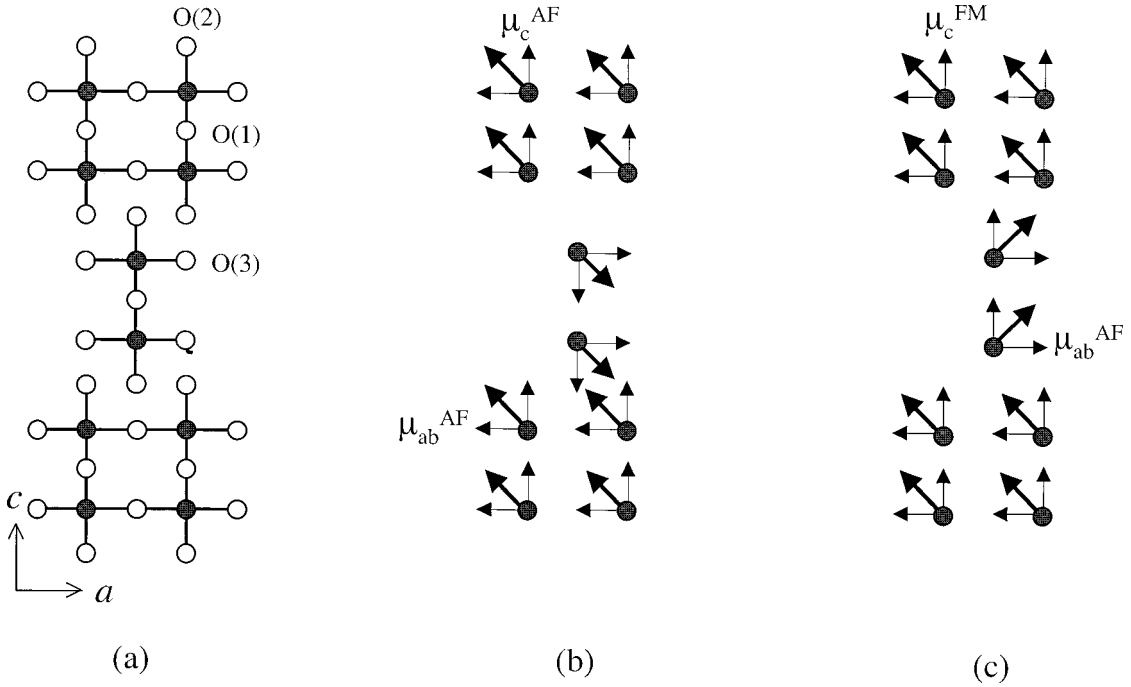


FIG. 5. (a) Crystal structure of $La_{2-2x}Sr_{1+2x}Mn_2O_7$. The three oxygen sites are labeled while the La,Sr atoms are not shown. (b) Arrangement of Mn spins depicting the antiferromagnetic components $\mu_c^{\mathrm{AF}}$ and $\mu_{ab}^{\mathrm{AF}}$ (tilted antiferromagnet) and (c) the ferromagnetic component, $\mu_c^{\mathrm{FM}}$ in a canted ferromagnetic arrangement.

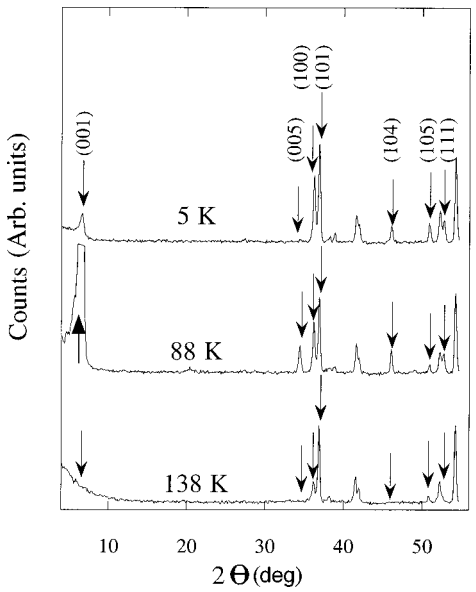


FIG. 6. Neutron powder-diffraction data measured at various temperatures above and below $T_{IM}$ from the $x=0.3$ sample, on the D20 diffractometer ($\lambda=2.41$ Å). Various FM and AF magnetic reflections are labeled.

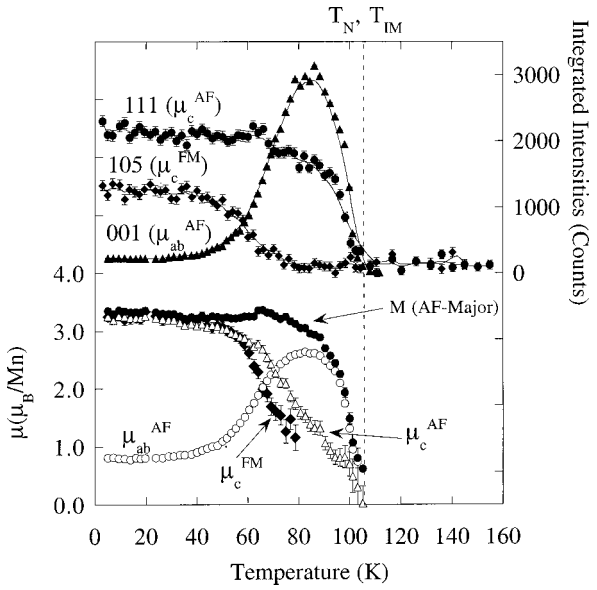


FIG. 7. Variation of intensities of the (111), (105), and (001) magnetic reflections as a function of temperature (upper portion). The (001) and (105) reflections represent directly the temperature dependence of the $\mu_{ab}^{AF}$ and $\mu_c^{FM}$ components, respectively, while the (111) represent a combination of $\mu_{ab}^{AF}$ and $\mu_c^{FM}$ components. The temperature dependence of the magnetic components $\mu_{ab}^{AF}$, $\mu_c^{AF}$, and $\mu_c^{FM}$ and the total moment $M$ in the AF majority phase are based on Rietveld refinement of data measured on the D20 diffractometer (lower portion).

antiferromagnetic metal with conduction through $d_{x^2-y^2}$ orbitals in layers separated by unoccupied $d_{3z^2-r^2}$ orbitals is clear.[5]

## IV. MAGNETIC STRUCTURE

The evolution of long-range magnetic order was studied using neutron powder diffraction on the D20. On cooling the sample, new magnetic reflections arise at $T_{IM}$ indicative of a long-range AF state (see Fig. 6). Reflections such as the (001) and (005) arise below 100 K from AF stacking along the *c* axis of FM perovskite bilayers with the Mn spins parallel to the *ab* plane, $\mu_{ab}^{AF}$. Also below 100 K the (100), (104), (111) reflections signal an AF ordering along the *c* axis of FM bilayers with the Mn spins parallel to the *c* axis, $\mu_c^{AF}$. These arrangements are shown schematically in Figs. 5(b) and 5(c). Inspection of the data revealed no signs of a FM stacking of FM in-plane moments, as seen in the $x=0.4$ composition.[4] In both cases the observed antiferromagnetic reflections are consistent with a spin arrangement where Mn moments order ferromagnetically *within* perovskite bilayers (*intrabilayer* coupling is FM), but rotate by 180° in the adjacent layer, forming an antiferromagnetic *interbilayer* coupling [see Fig. 5(b)]. The temperature dependence of the (111) and (001) reflections, characteristic of $\mu_c^{AF}$ and $\mu_{ab}^{AF}$, are shown in Fig. 7. We note that the component of the AF moment in the *ab* plane has a maximum in its temperature dependence at 80 K (see Fig. 7), indicating that the ordered moment rotates with cooling to form a tilted antiferromagnetic interbilayer coupling at low temperatures. This is the structure suggested by Kimura *et al.* from magnetization measurements,[2] and by Heffner *et al.* from $\mu$SR measurements.[15] A closer inspection of the diffraction data reveals additional intensity development on the (101), (105), and (110) nuclear reflections below 75 K. This extra intensity is consistent with a ferromagnetic arrangement of Mn spins aligned along the *c* axis $\mu_c^{FM}$ [see Fig. 5(c)]. The temperature dependence of the (105) reflection is also shown in Fig. 7. We emphasize that for the *c*-axis magnetic components $\mu_c^{FM}$ and $\mu_c^{AF}$, the perovskite bilayers remain ferromagnetically coupled; only the magnetic interbilayer coupling is different.

A determination of the low-temperature magnetic structure was attempted using a number of single magnetic phase models with different combinations of AF and FM components. Clearly, the coexistence of AF and FM *c*-axis magnetic components is not compatible with spin canting. Refinement of the diffraction data using combinations of FM and AF perovskite layers, produced intensity under the observed magnetic reflections, but the magnitude of the calculated intensities agreed poorly with the data. Also models where Mn moments were constrained to be different between adjacent layers (ferrimagnetic model) did not improve the fit further and in some cases led to divergent refinements. Furthermore, the absence of any superlattice reflections in the data eliminated models that include an ordered arrangement of FM and AF coupled bilayers along the *c* axis. We are thus led to conclude that the two magnetic components arise from distinct regions of the sample, each magnetically ordered over long length scales as indicated by resolution limited magnetic peak widths. This conclusion agrees with the results of the synchrotron x-ray study discussed above under the assumption that distinct chemical phases have distinct magnetic structures associated with them.

The magnetic structures observed here (AF interbilayer coupling and FM interbilayer coupling) have not been observed in any *single-phase* composition of the $La_{2-2x}Sr_{1+2x}Mn_2O_7$ system. However, a layered manganite

exhibiting a ferromagnetic structure with the Mn spins parallel to the $c$ axis is known for a doping level $x=0.32$.[16] Importantly, for $x>0.35$ FM moments are aligned parallel to the $ab$ plane.[16] This puts an upper concentration bound of $x=0.32$ on any possible phase separation in our nominal $x=0.3$ sample. Recent measurements on a $x=0.4$ bilayer sample give an estimate of the interbilayer exchange in this component as $J=0.065$ meV.[17] It is not unreasonable to speculate that the sign of such a small exchange (FM vs AF) could depend sensitively on the chemical environment. For single-phase samples of $x=0.32$, distinct ferromagnetic reflections appear at a $T_C$ of $\sim$125 K,[16] much higher than the 75 K where $c$-axis FM coupling is first clearly observed in the present nominally $x=0.3$ sample.

Good agreement with the neutron data at 5 K was found using models that included two distinct magnetic phases, consistent with the synchrotron x-ray results. In this analysis only one nuclear phase was included, as the phase separation behavior was not resolved on the D20. The assignment of the $c$-axis magnetic components is straightforward; the intensity of magnetic reflections arising from these $c$-axis components leads us to assign the $\mu_c^{\mathrm{AF}}$ to the major phase and $\mu_c^{\mathrm{FM}}$ to the minor phase. However, the assignment of the in-plane component is less clear. There are three possibilities: The in-plane AF component may be associated exclusively with the major phase (tilted AF structure), exclusively with the minor phase (canted FM structure), or divided between them (tilted AF structure+canted FM structure). Analysis of the data with $\mu_{ab}^{\mathrm{AF}}$ assigned exclusively to either the AF-major or the FM-minor phases lead to a refined total magnetic moment of 4.2 $\mu_B$/Mn at 80 K, substantially larger than the expected spin-only moment 3.7 $\mu_B$/Mn at this doping level. We thus take this as evidence that the in-plane component should be assigned to both major and minor phases.

With the available data we are not able to determine the relative contribution of the in-plane component in the two phases. To allow for this ambiguity, we have applied the following assumptions and/or constraints: (1) The saturation moment in both major and minor phases is the same ($\mu_{\mathrm{sat}}^{\mathrm{AF}}=\mu_{\mathrm{sat}}^{\mathrm{FM}}$). This assumption is valid because the small difference in the saturation moment due to composition ($\sim$0.02 $\mu_B$/Mn) is much smaller than the experimental error in determining the size of the Mn moment ($\sim 0.3\mu_B$/Mn). Application of this assumption allows us to determine the magnetic scale factor ($S$) at 5 K using the additional constraint of $S_{\mathrm{AF}}+S_{\mathrm{FM}}=S_{\mathrm{crystallographic}}$. Here $S_{\mathrm{AF}}$ is the Rietveld scale factor for the tilted AF phase [Fig. 5(b)], $S_{\mathrm{FM}}$ for the canted ferromagnetic phase [Fig. 5(c)] and $S_{\mathrm{crystallographic}}$ the chemical or nuclear only scale factor. (2) The magnitude of the in-plane component was constrained to be the same for both major and minor phases [$\mu_{ab}^{\mathrm{AF}}(\mathrm{major})=\mu_{ab}^{\mathrm{AF}}(\mathrm{minor})$]. This final constraint is arbitrary, but in the absence of additional information it is a simple, unbiased method of dividing the in-plane component between the two magnetic phases. Applying these constraints to the 5 K measurements, we obtain phase fractions of 62% (tilted AF phase) and 38% (canted FM phase). Given the difficulties of resolution, this result is in reasonable agreement with the ratio of major to minor chemical phases determined by the synchrotron x-ray measurements (75% and 25%). At 5 K the Rietveld analysis using these constraints yielded a saturation moment of 3.4(2) $\mu_B$/Mn, in excellent agreement with the bulk magnetization measurements of Kimura *et al.*[2] Although we acknowledge that the model just described is not unique, it does represent a good fit to the available low-temperature data and reproduces well the expected saturation moment at 5 K.

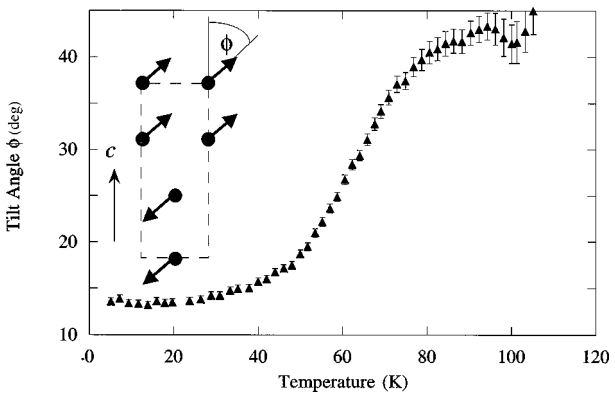


FIG. 8. Variation of the tilt angle $\phi$ as a function of temperature for the major phase in the nominal $x=0.3$ sample.

The results of the analysis of the temperature-dependent neutron-diffraction data are shown in Fig. 7. For this analysis the magnetic scale factors for the major and minor magnetic phases were fixed to the value determined at 5 K. This constraint reflects the assumption that the magnetic phases are tied to distinct chemical phases whose fractions will not vary in this temperature regime. As in the 5 K refinement, the magnitude of the in-plane component for both phases was constraint to be the same. The analysis under these constraints shows that at 100 K Mn spins in the majority phase—which exhibits AF *interbilayer* and FM *intrabilayer* coupling—order in a tilted arrangement with an angle $\phi\sim 43°$, from the $c$ axis. On cooling, Mn spins rotate towards the $c$ axis, reaching a final value of $\phi\sim 13°$ at 5 K (see Fig. 8). We note that in these analyses the total magnetization of the majority phase does not exceed the saturation moment at 80 K as occurred in a previously described model (see Fig. 7). The evolution of magnetic structure of the minor phase is similar to that of the major phase, except that no FM component is observed above 75 K. For the minor phase the data also suggest a transition from a canted to an almost colinear ferromagnetic state at 5 K. However, the analysis of the data using this model indicates that close to $T_{\mathrm{IM}}$, the magnetic ordering in the minor phase is purely AF in the $ab$ plane. That both major and minor phases exhibit a similar temperature dependence of their lattice parameter suggests that the minor phases also undergo a similar rotation in the direction of the Mn moment as the majority phase. If this is correct, then there will be a FM interbilayer component in the minority phase above 75 K. As ferromagnetic intensity appears superimposed on nuclear reflections, our sensitivity to this component is limited, particularly in a minority phase. Therefore at present we cannot rule out the possibility of a small ferromagnetic $c$-axis component ($\mu_c^{\mathrm{FM}}$) above 75 K in the minority phase.

## V. SUMMARY

In this paper we report on the structure and magnetism of the layered manganite $La_{2-2x}Sr_{1+2x}Mn_2O_7$ with nominal

composition $x=0.3$. Our sample exhibits a biphasic behavior corresponding to two layered manganite phases. The two phases show considerable similarity in terms of both composition ($\delta x \sim 0.02$) and lattice effects at $T_{IM}$. The lattice parameters of these two phases track one another in parallel with temperature—including the anomaly through the magnetic transition—indicating a similar charge spin-lattice coupling. We find that the main difference between these two phases lies in their magnetic structure, which exhibits a clear temperature dependence. At 5 K the majority phase exhibits AF interbilayer coupling, as suggested by other workers,[2,15] while the minority phase shows FM interbilayer coupling. It is interesting to note that despite the different *interbilayer* coupling, the lattice parameters of both phases parallel one another as a function of temperature. This suggests that the spin-lattice interaction is largely confined to the perovskite blocks and that interbilayer spin-lattice coupling is considerably weaker. Both x-ray and neutron results imply that the minority phase has a greater hole concentration than the majority phase, suggesting that hole-rich compositions favor FM interbilayer coupling. This is consistent with the broader picture of the $(La,Sr)_3Mn_2O_7$ phase diagram.[16] Structure and magnetism in this nominally $x=0.3$ sample are in sharp contrast to the prototypical layered ferromagnetic CMR manganite with composition $x=0.4$. We find structural behavior consistent with a model in which hole doping leads to changes in the charge transfer on cooling through $T_{IM}$ into $d_{3z^2-r^2}$ orbitals for $x=0.4$ and into $d_{x^2-y^2}$ orbitals for $x=0.3$. This demonstrates that the direction of lattice effects in layered materials is a sensitive function of charge and orbital degrees of freedom and implies a crossover between $x=0.3$ and $x=0.4$. Finally, these measurements also suggest that the interbilayer magnetic coupling is governed by charge and orbital degrees of freedom, since the easy axis varies from within the *ab* plane to along the *c* axis over the same compositional range as the crossover in lattice effects.

We thank R. B. von Dreele for allowing some preliminary powder-diffraction measurements on the HIPD spectrometer at the Manuel Lujan Jr. Neutron Scattering Center, Los Alamos National Laboratory. Preliminary neutron-scattering data from single crystals of $x=0.3$ were also measured on SCD at the Lujan center. We also thank R. Heffner and K. Gray for making available preprints of their work on these materials. This work was supported by the U. S. Department of Energy, Basic Energy Sciences-Materials Sciences under Contract No. W-7405-ENG-36 (D.N.A., H.N.B.), W-31-109-ENG-38 (J.F.M., J.D.J.) and DE-AC02-98CH10886 (D.E.C.), and UCDRD Grant No. STB-UC:97-240 (H.N.B.). D.N.A. also thanks the Institut Laue-Langevin for financial support.

[1] T. Kimura, Y. Tomioka, H. Kuwahara, A. Asamitsu, M. Tamura, and Y. Tokura, Science **274**, 1698 (1996).

[2] T. Kimura, A. Asamitsu, Y. Tomioka, and Y. Tokura, Phys. Rev. Lett. **79**, 3720 (1997).

[3] We note that apart from spin polarized tunneling the observed TMR in $La_{1.4}Sr_{1.6}Mn_2O_7$ may also arise in part from domain boundary effects.

[4] J. F. Mitchell, D. N. Argyriou, J. D. Jorgensen, D. G. Hinks, C. D. Potter, and S. D. Bader, Phys. Rev. B **55**, 63 (1997).

[5] T. Akimoto, Y. Maruyama, Y. Moritomo, A. Nakamura, K. Hirota, K. Ohoyama, and M. Ohashi, Phys. Rev. B **57**, 5594 (1998).

[6] Q. A. Li, K. E. Gray, and J. F. Mitchell, Phys. Rev. B (to be published).

[7] P. D. Battle, D. E. Cox, M. A. Green, J. E. Milburn, L. E. Spring, P. G. Radaelli, M. J. Rosseinsky, and J. F. Vente, Chem. Mater. **9**, 1042 (1997).

[8] P. G. Radaelli, D. E. Cox, M. Marezio, S.-W. Cheong, P. E. Schiffer, and A. P. Ramirez, Phys. Rev. Lett. **75**, 4488 (1995).

[9] V. Caignaert, E. Suard, A. Maignan, C. Simon, and B. Raveau, J. Magn. Magn. Mater. **153**, L260 (1996).

[10] D. N. Argyriou, J. F. Mitchell, C. D. Potter, S. D. Bader, R. Kleb, and J. D. Jorgensen, Phys. Rev. B **55**, 11 965 (1997).

[11] Since we cannot resolve the two layered structures that essentially differ only along the *c* axis, bond lengths obtained from Rietveld refinement represent only the weighted mean bond length between the major and the minor phases. The parallel temperature dependence of the lattice parameters [see Fig. 2(a)] indicates that the individual phases would behave qualitatively like the average of the two.

[12] D. Louca, G. H. Kwei, and J. F. Mitchell, Phys. Rev. Lett. **80**, 3811 (1998).

[13] D. S. Dessau, T. Saitoh, C. H. Park, Z. X. Shen, P. Villella, N. Hamada, Y. Moritomo, and Y. Tokura, Phys. Rev. Lett. **81**, 192 (1998).

[14] J.-S. Zhou, J. B. Goodenough, and J. F. Mitchell, Phys. Rev. B **58**, R579 (1998).

[15] R. H. Heffner, D. E. MacLaughlin, G. J. Nieuwenhuys, T. Kimura, G. M. Luke, Y. Tokura, and Y. J. Uemura, Phys. Rev. Lett. **81**, 1706 (1998).

[16] M. Medarde and J. F. Mitchell (private communication).

[17] S. Rosenkranz, R. Osborn, L. Vasiliu-Doloc, J. W. Lynn, S. K. Sinha, and J. F. Mitchell, Phys. Rev. Lett. **81**, 3964 (1998).